ResearchGate

See discussions, stats, and author profiles for this publication at: https://www.researchgate.net/publication/280966790

Strong Negative Temperature Dependence of the Simplest Criegee Intermediate CH2OO Reaction with Water Dimer

ARTICLE *in* JOURNAL OF PHYSICAL CHEMISTRY LETTERS · JULY 2015

Impact Factor: 7.46 · DOI: 10.1021/acs.jpclett.5b01109 · Source: PubMed

CITATION
1

READS
27

7 AUTHORS, INCLUDING:

Mica Smith
University of California, Berkeley
9 PUBLICATIONS **130** CITATIONS
SEE PROFILE

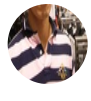

Chun-Hung Chang
University of Virginia
6 PUBLICATIONS **46** CITATIONS
SEE PROFILE

Kaito Takahashi
Academia Sinica
43 PUBLICATIONS **545** CITATIONS
SEE PROFILE

Jim J Lin
Academia Sinica
122 PUBLICATIONS **2,721** CITATIONS
SEE PROFILE

Available from: Mica Smith
Retrieved on: 30 January 2016

THE JOURNAL OF PHYSICAL CHEMISTRY Letters

Letter

pubs.acs.org/JPCL

Strong Negative Temperature Dependence of the Simplest Criegee Intermediate CH_2OO Reaction with Water Dimer

Mica C. Smith,[†,‡] Chun-Hung Chang,[‡] Wen Chao,[‡,§] Liang-Chun Lin,[‡,§] Kaito Takahashi,[‡] Kristie A. Boering,[†,∥] and Jim Jr-Min Lin*[,‡,§]

[†]Department of Chemistry, University of California, Berkeley, Berkeley, California 94720, United States

[‡]Institute of Atomic and Molecular Sciences, Academia Sinica, Taipei 10617, Taiwan

[§]Department of Chemistry, National Taiwan University, Taipei 10617, Taiwan

[∥]Department of Earth and Planetary Science, University of California, Berkeley, Berkeley, California 94720, United States

Supporting Information

ABSTRACT: The kinetics of the reaction of CH_2OO with water vapor was measured directly with UV absorption at temperatures from 283 to 324 K. The observed CH_2OO decay rate is second order with respect to the H_2O concentration, indicating water dimer participates in the reaction. The rate coefficient of the CH_2OO reaction with water dimer can be described by an Arrhenius expression $k(T) = A\exp(-E_a/RT)$ with an activation energy of -8.1 ± 0.6 kcal mol^{-1} and $k(298\text{ K}) = (7.4 \pm 0.6) \times 10^{-12}$ cm^3 s^{-1}. Theoretical calculations yield a large negative temperature dependence consistent with the experimental results. The temperature dependence increases the effective loss rate for CH_2OO by a factor of ~2.5 at 278 K and decreases by a factor of ~2 at 313 K relative to 298 K, suggesting that temperature is important for determining the impact of Criegee intermediate reactions with water in the atmosphere.

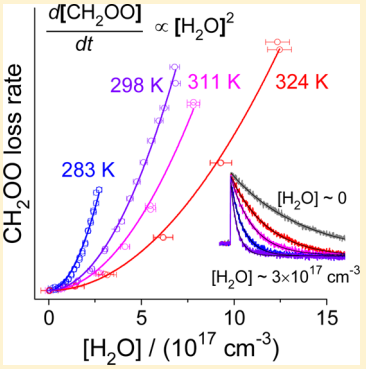

Downloaded by ACADEMIA SINICA on September 3, 2015 | http://pubs.acs.org
Publication Date (Web): June 26, 2015 | doi: 10.1021/acs.jpclett.5b01109

Criegee intermediates (CIs), including CH_2OO and other substituted carbonyl oxides, form in the atmosphere primarily via reactions between ozone and unsaturated hydrocarbons (ozonolysis). CIs are thought to play a significant role in the oxidizing capacity of the atmosphere, as evidenced by studies connecting ozonolysis products to OH and H_2SO_4 formation as well as aerosol growth.[1−6] Determining the rates and mechanisms of the reactions of CIs with water vapor is necessary to evaluate the relative influence of various CIs on the production of atmospheric oxidants and aerosol precursors, e.g., from reactions with SO_2 and NO_2, since the reactions of CIs with water compete with these other processes.

Investigations of CH_2OO formed by C_2H_4 ozonolysis typically use indirect methods to measure the reaction kinetics (i.e., rate determinations are made relative to a reaction with a known rate or by detection of the product of another CH_2OO reaction). These methods have yielded a wide range of values for the rate coefficient of CH_2OO reaction with water, from 10^{-17} to 10^{-12} cm^3 s^{-1}.[7−10] Recently, Berndt et al.[11] measured competing reactions for CH_2OO from C_2H_4 ozonolysis at high water concentrations and observed second-order kinetics with regard to $[H_2O]$ for CH_2OO loss, signifying a fast rate of CH_2OO reaction with $(H_2O)_2$. They estimated the $CH_2OO + (H_2O)_2$ rate coefficient, k_{dimer}, to be ~1.1×10^{-11} cm^{3}s^{-1}, and suggested that discrepancies among experiments may be due to differences in the water vapor concentrations, since the effect of $(H_2O)_2$ on the reaction rates will depend on the $[H_2O]$ used in the experiments.[11]

The method introduced by Welz et al.[12] to produce detectable levels of stabilized CIs (from photolysis of diiodoalkanes in O_2) has prompted many studies reporting direct measurements of CIs, leading to new insights into their structures and reactivities.[13−21] CH_2OO, the simplest CI, has been investigated extensively using the reaction schemes $CH_2I_2 + h\nu \rightarrow CH_2I + I$ and $CH_2I + O_2 \rightarrow CH_2OO + I$. Investigations of the CH_2I_2/O_2 photolysis system, utilizing photoionization mass spectrometry[12] and UV, IR, and microwave spectroscopy,[16,17,22] indicate that CH_2OO is the predominant isomer formed. Studies of CH_2OO reaction kinetics using this scheme show that CH_2OO reacts rapidly with SO_2, NO_2, and some atmospheric organic compounds.[12,23−26] Notably, the reaction of CH_2OO with SO_2 has a large rate coefficient of $(3.9 \pm 0.7) \times 10^{-11}$ cm^3 s^{-1} determined by Welz et al.[12] By contrast, the reaction of CH_2OO with H_2O was not detectable in that study, and an upper limit of 4×10^{-15} cm^3 s^{-1} was given for the rate coefficient.[12] As stated by Berndt et al.,[11] the H_2O concentrations in the Welz et al. experiment were too low ($\lesssim 3 \times 10^{16}$ cm^{-3}) to reveal the effect of water dimer on the CH_2OO loss rates. However, relative rate studies of CH_2OO from CH_2I_2 photolysis performed by Stone et al.[23] and by Ouyang et al.[26] at higher H_2O concentrations also yielded small rate coefficients below 1×10^{-16} cm^3 s^{-1}, a discrepancy that

Received: May 27, 2015
Accepted: June 24, 2015
Published: June 24, 2015

© 2015 American Chemical Society

DOI: 10.1021/acs.jpclett.5b01109
J. Phys. Chem. Lett. 2015, 6, 2708−2713

Downloaded by ACADEMIA SINICA on September 3, 2015 | http://pubs.acs.org
Publication Date (Web): June 26, 2015 | doi: 10.1021/acs.jpclett.5b01109

could not be explained by Berndt and co-workers.[11] Very recently, Chao et al.[27] used the strong UV absorption of CH_2OO at 340 nm[17] to measure the kinetics of CH_2OO reaction with water vapor at high water concentrations. Clear second-order kinetics with respect to $[H_2O]$ were observed, providing direct evidence for the fast reaction with water dimer. The value reported by Chao et al.[27] for k_{dimer} at 298 K, $(6.5 \pm 0.8) \times 10^{-12}$ cm^3 s^{-1}, is about half the value from the Berndt et al. study (which used a slightly different temperature of 293 K and a different source for the water dimer equilibrium constants)[11] but within 2σ of $k_{dimer}(298\ K) = (4.0 \pm 1.2) \times 10^{-12}$ cm^3 s^{-1} determined by Lewis et al. using a similar direct CH_2OO UV absorption method.[28] Chao et al.[27] proposed that interferences to the detected signal from products of the reaction of CH_2OO with water could account for the slower apparent rates reported by Stone et al.[23] and Ouyang et al.[26]

Given that the k_{dimer} value is on the order of 10^{-12} cm^3 s^{-1}, the reaction with water dimer would be the main pathway for atmospheric CH_2OO loss since the concentration of $(H_2O)_2$ in the troposphere is on the order of 10^{14} cm^{-3}, much higher than those of other potential reactants like SO_2, NO_2, and organic compounds. The fast reaction rate of CH_2OO with water dimer will lead to a low steady state concentration of CH_2OO in the troposphere. However, because temperature and humidity can vary widely both regionally and seasonally, the actual loss rate of CH_2OO due to reaction with water vapor could potentially depend strongly on atmospheric conditions. To better understand the atmospheric impact and mechanism of the CH_2OO reaction with water dimer, we measured the transient absorption of CH_2OO as a function of temperature and H_2O concentration and compared the temperature-dependent rate coefficient with quantum chemical calculations.

Representative difference transient absorption traces under dry (without adding water) and wet (with water vapor added) conditions at 283, 298, 311, and 324 K are shown in Figure 1. The rapid increase in absorption after the photolysis laser pulse at time = 0 (photolyzing CH_2I_2 in the reactor to generate CH_2I) corresponds to CH_2OO formation from $CH_2I + O_2$, and the subsequent decrease in absorption over several milliseconds is attributed to CH_2OO loss. Under dry conditions, the decay in CH_2OO absorption is due primarily to CH_2OO reactions with radical species, including I atoms, CH_2IOO, and CH_2OO,[29] while under wet conditions CH_2OO reaction with water dominates the observed decay. We found the change in CH_2OO concentration with time t can be described by kinetic eqs 1 and 2 in which k_{obs} is the sum of the dry loss rate, k_0, and the loss rate due to reaction with water vapor, k_w', similar to Chao et al.;[27] the transient absorption traces were fit to a single exponential decay to yield the decay constant k_{obs}.

$$-\frac{d[CH_2OO]}{dt} = k_0[CH_2OO] + k_w'[CH_2OO] = k_{obs}[CH_2OO] \quad (1)$$

$$[CH_2OO]_t = [CH_2OO]_0 \exp(-k_{obs}t) \quad (2)$$

The reaction kinetics of CH_2OO in the $CH_2I + O_2$ reaction system has been investigated by Ting et al.[29] In eq 1, the $k_0[CH_2OO]$ term includes contributions from several reactions including $CH_2OO + CH_2OO \rightarrow$ products; $CH_2OO + I + M \rightarrow CH_2IO_2 + M$; $CH_2OO + I \rightarrow IO + CH_2O$; and $CH_2OO + CH_2IO_2 \rightarrow$ products. Under our experimental conditions of high pressures and low CH_2OO concentrations, the self-reaction of CH_2OO is not expected to dominate in the $[CH_2OO]$ decay;[29] this assumption is supported by the pseudo-first-order kinetics of the observed decay. Furthermore, to the best of our knowledge, there is no evidence that the contributions of the above reactions depend on water concentration. Sheps et al.[30] measured the kinetics of the reaction of *syn*-CH_3CHOO with water, which was found to be very slow; their plot of k_{obs} as a function of $[H_2O]$ has a zero slope, suggesting that k_0 for the syn-CH_3CHOO reaction with water does not depend on $[H_2O]$. Here we assume that k_0 for CH_2OO reaction with water is also independent of $[H_2O]$ and that eq 1 is valid under our conditions.

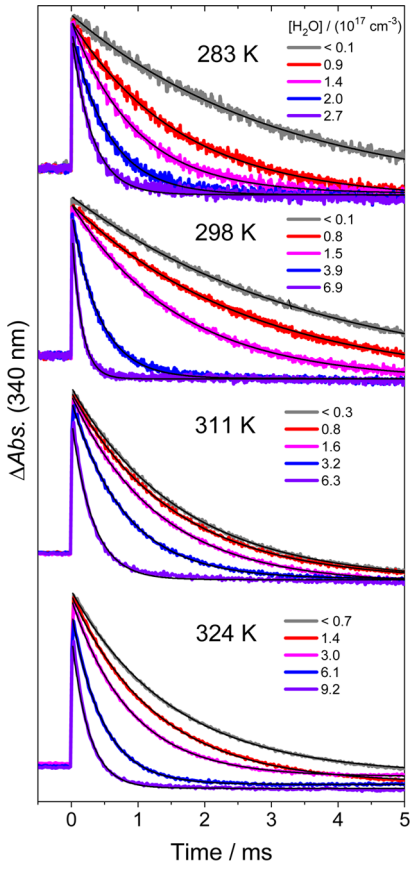

Figure 1. Difference transient absorbance traces at 340 nm showing CH_2OO formation and decay at four temperatures, with total pressure P_{total} = 500–600 Torr. Gray traces correspond to dry conditions (no H_2O added) and colored traces correspond to absorbance at different H_2O concentrations. Note that different water concentrations were used for experiments at different temperatures. Black lines are the single exponential fits. The negative baseline at long delay times is attributed to the depletion of the CH_2I_2 precursor, which absorbs weakly at 340 nm. The depletion of CH_2I_2 is a step function[29] and does not affect our rate analysis.

Under dry conditions, our $k_{obs} = k_0$; subtracting k_0 from k_{obs} yields k_w' at different water concentrations, which are plotted in Figure 2. The relationship between k_w' and $[H_2O]$ at all studied temperatures is second order, suggesting the observed CH_2OO loss is dominated by reaction with water dimer.[27] It is clear that the CH_2OO decay rates at higher temperatures are significantly slower for a given H_2O concentration.

The second-order kinetics with regard to $[H_2O]$ indicates that k_w' can be fit to a linear relationship with $[(H_2O)_2]$ as shown in Figure 2, in which the slope corresponds to $k_{dimer}(T)$ (see eq 3). Expression 4 is used to determine $[(H_2O)_2]$ at a

DOI: 10.1021/acs.jpclett.5b01109
J. Phys. Chem. Lett. 2015, 6, 2708–2713

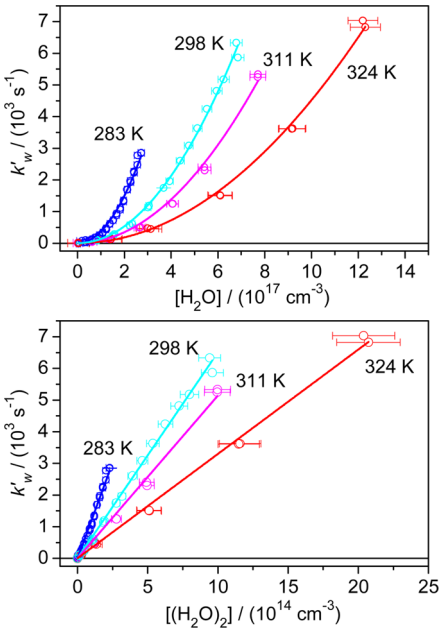

Figure 2. Pseudo-first-order CH_2OO loss rate coefficients k_w' plotted against H_2O concentration (top) and $(H_2O)_2$ concentration (bottom). The curves and lines are quadratic and linear fits to the data, respectively.

given temperature, in which $K_{eq}(T)$ is the temperature-dependent equilibrium constant for water dimerization. We use the $K_{eq}(T)$ values reported by Ruscic,[31] who utilized the Active Thermochemical Tables approach; the reported uncertainties range from 2.9 to 3.3% in the temperature range studied here. The following k_{dimer} values were obtained by averaging the slopes from all experiments at each temperature: k_{dimer} /(10^{-12} cm^3 s^{-1}) = 12.1 ± 1.7, 7.4 ± 0.6, 4.8 ± 0.5, 3.3 ± 0.7 for 283, 298, 311, 324 K, respectively.

$$(k_{obs} - k_0) = k'_w = k_{dimer}(T)[(H_2O)_2] \quad (3)$$

$$K_{eq}(T) = \frac{[(H_2O)_2]}{[H_2O]^2} \quad (4)$$

The $k_{dimer}(T)$ values obtained from each experiment described above are plotted (triangles) in the Arrhenius plot in Figure 3. CH_2OO transient absorption was also measured at constant $[H_2O]$ = (5.4 ± 0.3) × 10^{17} cm^{-3} at a series of temperatures from 298 to 324 K (total pressure = 200−600 Torr; no pressure dependence was observed). Dividing $k_w'(T)$ by $[(H_2O)_2]$ yields k_{dimer} as a function of temperature; these values are plotted (squares) in Figure 3. Fitting the data from this experiment to the Arrhenius form $k(T) = A\exp(-E_a/RT)$ gives a value of −8.1 ± 0.6 kcal mol^{-1} for E_a.

This negative temperature dependence may be explained by a complex-formation reaction mechanism. A previous theoretical analysis[32] predicted that at thermal equilibrium the observed temperature dependence of k_{dimer} should be influenced by the temperature dependence of the equilibrium between reactants and prereactive complexes as well as the temperature dependence of the rate coefficient for the complex crossing the transition state to products. Our k_{dimer} does not show any pressure dependence from 100 to 600 Torr (see Supporting Information and ref 27), signifying that our experimental conditions are at the high pressure limit and that reactants and prereactive complexes have reached thermal equilibrium before

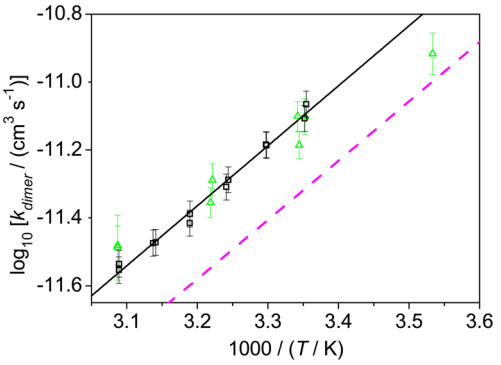

Figure 3. Arrhenius plot of k_{dimer}. Triangles represent k_{dimer} obtained by varying the water dimer concentrations at fixed temperatures (experiments #1−3; see Table S1). Squares represent k_{dimer} obtained by varying T (298−324 K) at constant $[H_2O]$ (experiment #6). Solid line is a linear fit to data from experiment #6. Dashed pink line shows the calculated $k_{dimer}(T)$.

the reaction takes place. To gain more insight into the reaction mechanism, we used transition state theory and high-level ab initio quantum chemistry to calculate $k_{dimer}(T)$ in the experimental temperature range. The relevant potential energy surface is shown in Figure S12. Figure 3 shows that the calculated $k_{dimer}(T)$ exhibits a negative temperature dependence with a slope that is similar to the experiment, though the calculation slightly underestimates (by ∼30%) the absolute magnitude of the rate coefficients. This slope is attributed to (1) the large dipole moment of CH_2OO, which causes strong interaction with water dimer, and (2) the small geometry change between the complex and the transition state. The former leads to a large binding energy of the prereactive complex $CH_2OO\cdot(H_2O)_2$, around 11 kcal mol^{-1}, while the latter causes the reaction barrier to be very low, around 5 kcal mol^{-1}. As a result, the transition state energy lies below the energy of the reactants $CH_2OO+(H_2O)_2$ by about 6 kcal mol^{-1}. Note that the $CH_2OO\cdot(H_2O)_2$ complex may also form via $CH_2OO\cdot H_2O + H_2O$, but this pathway would not change our theoretical results as long as $CH_2OO\cdot(H_2O)_2$ and the reactants are in thermal equilibrium. The agreement between theory and experiment for the title reaction may allow us to use theory to predict the temperature dependences of water dimer reactions with other CIs.

Few other examples exist for such a large negative E_a in a gas-phase reaction near room temperature. An activation energy around −13 kcal mol^{-1} has been observed in the reaction of SO_3 with H_2O, attributed primarily to the formation of stable prereactive complexes involving $(H_2O)_2$.[33−36] The results presented here for CH_2OO reaction with water dimer imply that the stability of prereactive complexes between larger CIs and $(H_2O)_2$ may be a key factor controlling the temperature dependences of their reactions with water vapor.

The temperature dependence of k_{dimer} indicates that CH_2OO loss due to reaction with water vapor will be sensitive to ambient temperatures in the atmosphere. The effective first-order CH_2OO loss rate coefficient, $k_{eff} = k_{dimer}(T)[(H_2O)_2]$, depends strongly on atmospheric temperature and relative humidity RH; this will influence the steady state concentrations of CH_2OO in the atmosphere, which in turn influence CH_2OO reaction rates with other species such as SO_2.[27] For example, using the temperature dependence of k_{dimer} obtained in this work gives $k_{eff}(T = 278$ K, RH = 70%) = 1570 s^{-1} ([$(H_2O)_2$] =

Downloaded by ACADEMIA SINICA on September 3, 2015 | http://pubs.acs.org
Publication Date (Web): June 26, 2015 | doi: 10.1021/acs.jpclett.5b01109

DOI: 10.1021/acs.jpclett.5b01109
J. Phys. Chem. Lett. 2015, 6, 2708−2713

7.5×10^{13} cm^{-3}) and k_{eff}(313 K, 30%) = 1900 s^{-1} ($[(H_2O)_2]$ = 4.2×10^{14} cm^{-3}), while ignoring the temperature dependence would lead to k_{eff}(278 K, 70%) = 590 s^{-1} and k_{eff}(313 K, 30%) = 3670 s^{-1}.

In summary, transient absorption measurements of CH_2OO at high concentrations of water vapor from 283 to 324 K reveal a pronounced negative temperature dependence of the rate coefficient for the reaction of CH_2OO with water dimer, and are consistent with theoretical calculations that predict prereactive complexes in the reaction mechanism. The strong dependence of the reaction of the simplest CI CH_2OO with water vapor on atmospheric temperature and humidity emphasizes the importance of investigating the reactions of larger CIs with water. Different CIs are likely to display different degrees of temperature dependence, and accurate knowledge of these differences will help constrain the relative importance of various decay pathways of CIs and their influence on atmospheric composition. Since there is currently no method available to measure the concentrations of CIs in the atmosphere, the concentration of atmospheric CH_2OO (as well as concentrations of other CIs) must be estimated from known rates of production and removal. While the rates of production of some CIs can be determined from available ozonolysis rates and CI yields, the rates of CI removal remain highly uncertain. The results presented here will help to constrain CH_2OO removal rates under different atmospheric conditions, a critical step toward understanding the impact of CIs on the atmosphere's oxidizing capacity.

EXPERIMENTAL AND COMPUTATIONAL METHODS

The experimental apparatus has been described previously.[17,20,27,37] In brief, the N_2 carrier gas is premixed with O_2, CH_2I_2, and water vapor in Teflon tubes and enters a ~76 cm long photolysis reactor; 248 nm light from an excimer laser photodissociates CH_2I_2 and induces formation of CH_2OO, which is monitored continuously in real time by its strong absorption at 340 nm. A broadband plasma light source (Energetic, EQ99) is directed through the reactor in a multiple-pass configuration (6 or 8 passes) to increase the absorption signal, which is measured by a balanced photodiode detector (Thorlabs, PDB450A) through a 335−345 nm bandpass filter. For this work, the photolysis reactor was immersed in a temperature-controlled circulating water bath. The measured temperature stability was better than ±0.3 K (with accuracy better than ±0.6 K) for all experiments.

The temperature dependent equilibrium constants for van der Waals (VDW) complex formation and rate coefficients for crossing the transition state (TS) in the reaction between CH_2OO and water dimer were calculated using the THERMO, ADENSUM, LAMM, and SCTST programs in the Multiwell suite.[38−44] The relative energies for the reactants, VDW complexes, TSs and the product were obtained by complete basis set extrapolation using the QCISD(T)[45] method with the Dunning basis[46] at the geometries calculated by B3LYP[47,48]/6-311+G(2d,2p).[49−51] To confirm the B3LYP geometries, geometry optimization was also performed using QCISD(T)/6-311+G(2d,2p) for one of the reaction paths. In addition, harmonic frequencies and anharmonic corrections within the vibrational second-order perturbation theory were obtained at the B3LYP level. All the B3LYP and QCISD(T) calculations were performed using the Gaussian09[52] and MOLPRO[53] program, respectively.

Previously, Ariya and co-workers[32,54,55] found two TSs leading to the product hydroxymethyl hydroperoxide (HMHP) water cluster. In this work, four TSs were found to lead to the HMHP water cluster. Two of the four are equivalent to those obtained by Ariya et al.,[32,54,55] while the other two were obtained by internal rotation of the free OH bonds of the water. Four different reactant VDW complexes were obtained from the four TSs. Following the previous work by Ariya and co-workers,[32] the rate constants $k_{dimer}(T)$ were calculated assuming (1) that thermal equilibrium is reached between the reactant and VDW complex, (2) that a steady state approximation is valid for the VDW complex, and (3) that the four TSs for the dimer reaction are independent. Therefore, the dimer rate constant for each reaction path is calculated as the product of the equilibrium constant for VDW complex formation and the rate constant for the VDW reaction to form HMHP. The total dimer rate constant is obtained by adding up the rates from the four pathways.

More details on experimental and computational methods are available in the Supporting Information.

ASSOCIATED CONTENT

Supporting Information

Experimental and theoretical methods, supplementary figures and tables. The Supporting Information is available free of charge on the ACS Publications website at DOI: 10.1021/acs.jpclett.5b01109.

AUTHOR INFORMATION

Corresponding Author

*E-mail: jimlin@gate.sinica.edu.tw.

Notes

The authors declare no competing financial interest.

ACKNOWLEDGMENTS

This research was supported by Academia Sinica and the Ministry of Science and Technology of Taiwan (MOST103-2113-M-001-019-MY3; 102-2113-M-001-012-MY3).

REFERENCES

(1) Heard, D. E.; Carpenter, L. J.; Creasey, D. J.; Hopkins, J. R.; Lee, J. D.; Lewis, A. C.; Pilling, M. J.; Seakins, P. W.; Carslaw, N.; Emmerson, K. M. High Levels of the Hydroxyl Radical in the Winter Urban Troposphere. *Geophys. Res. Lett.* **2004**, *31*, 1−5, DOI: 10.1029/2004GL020544.

(2) Emmerson, K. M.; Carslaw, N.; Pilling, M. J. Urban Atmospheric Chemistry during the PUMA Campaign 2: Radical Budgets for OH, HO_2 and RO_2. *J. Atmos. Chem.* **2005**, *52*, 165−183, DOI: 10.1007/s10874-005-1323-2.

(3) Mauldin, R. L., III; Berndt, T.; Sipilä, M.; Paasonen, P.; Petäjä, T.; Kim, S.; Kurtén, T.; Stratmann, F.; Kerminen, V.-M.; Kulmala, M. A New Atmospherically Relevant Oxidant of Sulphur Dioxide. *Nature* **2012**, *488*, 193−196, DOI: 10.1038/nature11278.

(4) Ehn, M.; Thornton, J. A.; Kleist, E.; Sipilä, M.; Junninen, H.; Pullinen, I.; Springer, M.; Rubach, F.; Tillmann, R.; Lee, B.; et al. A Large Source of Low-Volatility Secondary Organic Aerosol. *Nature* **2014**, *506*, 476−479, DOI: 10.1038/nature13032.

(5) Berresheim, H.; Adam, M.; Monahan, C.; O'Dowd, C.; Plane, J. M. C.; Bohn, B.; Rohrer, F. Missing SO_2 Oxidant in the Coastal Atmosphere? − Evidence from High Resolution Measurements of OH and Atmospheric Sulfur Compounds. *Atmos. Chem. Phys. Discuss.* **2014**, *14*, 1159−1190, DOI: 10.5194/acpd-14-1159-2014.

(6) Sarwar, G.; Simon, H.; Fahey, K.; Mathur, R.; Goliff, W. S.; Stockwell, W. R. Impact of Sulfur Dioxide Oxidation by Stabilized

Downloaded by ACADEMIA SINICA on September 3, 2015 | http://pubs.acs.org
Publication Date (Web): June 26, 2015 | doi: 10.1021/acs.jpclett.5b01109

DOI: 10.1021/acs.jpclett.5b01109
J. Phys. Chem. Lett. 2015, 6, 2708−2713

Downloaded by ACADEMIA SINICA on September 3, 2015 | http://pubs.acs.org
Publication Date (Web): June 26, 2015 | doi: 10.1021/acs.jpclett.5b01109

Criegee Intermediate on Sulfate. *Atmos. Environ.* **2014**, *85*, 204−214, DOI: 10.1016/j.atmosenv.2013.12.013.
(7) Suto, M.; Manzanares, E. R.; Lee, L. C. Detection of Sulfuric Acid Aerosols by Ultraviolet Scattering. *Environ. Sci. Technol.* **1985**, *19*, 815−820, DOI: 10.1021/es00139a008.
(8) Becker, K. H.; Bechara, J.; Brockmann, K. J. Studies on the Formation of H_2O_2 in the Ozonolysis of Alkenes. *Atmos. Environ.* **1993**, *27A*, 57−61, DOI: 10.1016/0960-1686(93)90070-F.
(9) Leather, K. E.; McGillen, M. R.; Cooke, M. C.; Utembe, S. R.; Archibald, A. T.; Jenkin, M. E.; Derwent, R. G.; Shallcross, D. E.; Percival, C. J. Acid-Yield Measurements of the Gas-Phase Ozonolysis of Ethene as a Function of Humidity Using Chemical Ionisation Mass Spectrometry (CIMS). *Atmos. Chem. Phys.* **2012**, *12*, 469−479, DOI: 10.5194/acp-12-469-2012.
(10) Newland, M. J.; Rickard, A. R.; Alam, M. S.; Vereecken, L.; Muñoz, A.; Ródenas, M.; Bloss, W. J. Kinetics of Stabilised Criegee Intermediates Derived from Alkene Ozonolysis: Reactions with SO_2, H_2O and Decomposition under Boundary Layer Conditions. *Phys. Chem. Chem. Phys.* **2015**, *17*, 4076−4088, DOI: 10.1039/C4CP04186K.
(11) Berndt, T.; Voigtländer, J.; Stratmann, F.; Junninen, H.; Mauldin, R. L.; Sipilä, M.; Kulmala, M.; Herrmann, H. Competing Atmospheric Reactions of CH_2OO with SO_2 and Water Vapour. *Phys. Chem. Chem. Phys.* **2014**, *16*, 19130−19136, DOI: 10.1039/C4CP02345E.
(12) Welz, O.; Savee, J. D.; Osborn, D. L.; Vasu, S. S.; Percival, C. J.; Shallcross, D. E.; Taatjes, C. A. Direct Kinetic Measurements of Criegee Intermediate (CH_2OO) Formed by Reaction of CH_2I with O_2. *Science* **2012**, *335*, 204−207, DOI: 10.1126/science.1213229.
(13) Taatjes, C. A.; Shallcross, D. E.; Percival, C. J. Research Frontiers in the Chemistry of Criegee Intermediates and Tropospheric Ozonolysis. *Phys. Chem. Chem. Phys.* **2014**, *16*, 1704−1718, DOI: 10.1039/c3cp52842a.
(14) Taatjes, C. A.; Welz, O.; Eskola, A. J.; Savee, J. D.; Scheer, A. M.; Shallcross, D. E.; Rotavera, B.; Lee, E. P. F.; Dyke, J. M.; Mok, D. K. W.; et al. Direct Measurements of Conformer-Dependent Reactivity of the Criegee Intermediate CH_3CHOO. *Science* **2013**, *340*, 177−180, DOI: 10.1126/science.1234689.
(15) Su, Y.-T.; Lin, H.-Y.; Putikam, R.; Matsui, H.; Lin, M. C.; Lee, Y.-P. Extremely Rapid Self-Reaction of the Simplest Criegee Intermediate CH_2OO and Its Implications in Atmospheric Chemistry. *Nat. Chem.* **2014**, *6*, 477−483, DOI: 10.1038/nchem.1890.
(16) Su, Y.-T.; Huang, Y.-H.; Witek, H. A.; Lee, Y.-P. Infrared Absorption Spectrum of the Simplest Criegee Intermediate CH_2OO. *Science* **2013**, *340*, 174−176, DOI: 10.1126/science.1234369.
(17) Ting, W.-L.; Chen, Y.-H.; Chao, W.; Smith, M. C.; Lin, J. J.-M. The UV Absorption Spectrum of the Simplest Criegee Intermediate CH_2OO. *Phys. Chem. Chem. Phys.* **2014**, *16*, 10438−10443, DOI: 10.1039/c4cp00877d.
(18) Beames, J. M.; Liu, F.; Lu, L.; Lester, M. I. Ultraviolet Spectrum and Photochemistry of the Simplest Criegee Intermediate CH_2OO. *J. Am. Chem. Soc.* **2012**, *134*, 20045−20048, DOI: 10.1021/ja310603j.
(19) Sheps, L. Absolute Ultraviolet Absorption Spectrum of a Criegee Intermediate CH_2OO. *J. Phys. Chem. Lett.* **2013**, *4*, 4201−4205, DOI: 10.1021/jz402191w.
(20) Smith, M. C.; Ting, W.-L.; Chang, C.-H.; Takahashi, K.; Boering, K. A.; Lin, J. J.-M. UV Absorption Spectrum of the C2 Criegee Intermediate CH_3CHOO. *J. Chem. Phys.* **2014**, *141*, 074302 DOI: 10.1063/1.4892582.
(21) Liu, F.; Beames, J. M.; Green, A. M.; Lester, M. I. UV Spectroscopic Characterization of Dimethyl- and Ethyl-Substituted Carbonyl Oxides. *J. Phys. Chem. A* **2014**, *118*, 2298−2306, DOI: 10.1021/jp412726z.
(22) Nakajima, M.; Endo, Y. Communication: Determination of the Molecular Structure of the Simplest Criegee Intermediate CH_2OO. *J. Chem. Phys.* **2013**, *139*, DOI:10.1063/1.4821165.
(23) Stone, D.; Blitz, M.; Daubney, L.; Howes, N. U. M.; Seakins, P. Kinetics of CH_2OO Reactions with SO_2, NO_2, NO, H_2O and CH_3CHO as a Function of Pressure. *Phys. Chem. Chem. Phys.* **2014**, *16*, 1139−1149, DOI: 10.1039/c3cp54391a.
(24) Buras, Z. J.; Elsamra, R. M. I.; Jalan, A.; Middaugh, J. E.; Green, W. H. Direct Kinetic Measurements of Reactions between the Simplest Criegee Intermediate CH_2OO and Alkenes. *J. Phys. Chem. A* **2014**, *118*, 1997−2006, DOI: 10.1021/jp4118985.
(25) Welz, O.; Eskola, A. J.; Sheps, L.; Rotavera, B.; Savee, J. D.; Scheer, A. M.; Osborn, D. L.; Lowe, D.; Murray Booth, A.; Xiao, P.; et al. Rate Coefficients of C1 and C2 Criegee Intermediate Reactions with Formic and Acetic Acid near the Collision Limit: Direct Kinetics Measurements and Atmospheric Implications. *Angew. Chemie - Int. Ed.* **2014**, *53*, 4547−4550, DOI: 10.1002/anie.201400964.
(26) Ouyang, B.; McLeod, M. W.; Jones, R. L.; Bloss, W. J. NO_3 Radical Production from the Reaction between the Criegee Intermediate CH_2OO and NO_2. *Phys. Chem. Chem. Phys.* **2013**, *15*, 17070 DOI: 10.1039/C3CP53024H.
(27) Chao, W.; Hsieh, J.-T.; Chang, C.-H.; Lin, J. J.-M. Direct Kinetic Measurement of the Reaction of the Simplest Criegee Intermediate with Water Vapor. *Science* **2015**, *347*, 751−754, DOI: 10.1126/science.1261549.
(28) Lewis, T. R.; Blitz, M. A.; Heard, D. E.; Seakins, P. W. Direct Evidence for a Substantive Reaction between the Criegee Intermediate, CH_2OO, and the Water Vapour Dimer. *Phys. Chem. Chem. Phys.* **2015**, *17*, 4859−4863, DOI: 10.1039/C4CP04750H.
(29) Ting, W.-L.; Chang, C.-H.; Lee, Y.-F.; Matsui, H.; Lee, Y.-P.; Lin, J. J.-M. Detailed Mechanism of the $CH_2I + O_2$ Reaction: Yield and Self-Reaction of the Simplest Criegee Intermediate CH_2OO. *J. Chem. Phys.* **2014**, *141*, 104308 DOI: 10.1063/1.4894405.
(30) Sheps, L.; Scully, A. M.; Au, K. UV Absorption Probing of the Conformer-Dependent Reactivity of a Criegee Intermediate CH_3CHOO. *Phys. Chem. Chem. Phys.* **2014**, *16*, 26701−26706, DOI: 10.1039/C4CP04408H.
(31) Ruscic, B. Active Thermochemical Tables: Water and Water Dimer. *J. Phys. Chem. A* **2013**, *117*, 11940−11953, DOI: 10.1021/jp403197t.
(32) Ryzhkov, A. B.; Ariya, P. A. A Theoretical Study of the Reactions of Parent and Substituted Criegee Intermediates with Water and the Water Dimer. *Phys. Chem. Chem. Phys.* **2004**, *6*, 5042 DOI: 10.1039/b408414d.
(33) Lovejoy, E. R.; Hanson, D. R.; Huey, L. G. Kinetics and Products of the Gas-Phase Reaction of SO_3 with Water. *J. Phys. Chem.* **1996**, *100*, 19911−19916, DOI: 10.1021/jp962414d.
(34) Kolb, C. E.; Jayne, J. T.; Worsnop, D. R.; Molina, M. J.; Meads, R. F.; Viggiano, A. A. Gas Phase Reaction of Sulfur Trioxide with Water Vapor. *J. Am. Chem. Soc.* **1994**, *116*, 10314−10315, DOI: 10.1021/ja00101a067.
(35) Jayne, J. T.; Pöschl, U.; Chen, Y.; Dai, D.; Molina, L. T.; Worsnop, D. R.; Kolb, C. E.; Molina, M. J. Pressure and Temperature Dependence of the Gas-Phase Reaction of SO_3 with H_2O and the Heterogeneous Reaction of SO_3 with H_2O/H_2SO_4 Surfaces. *J. Phys. Chem. A* **1997**, *101*, 10000−10011, DOI: 10.1021/jp972549z.
(36) Larson, L. J.; Kuno, M.; Tao, F.-M. Hydrolysis of Sulfur Trioxide to Form Sulfuric Acid in Small Water Clusters. *J. Chem. Phys.* **2000**, *112*, 8830 DOI: 10.1063/1.481532.
(37) Su, M.-N.; Lin, J. J.-M. Note: A Transient Absorption Spectrometer Using an Ultra Bright Laser-Driven Light Source. *Rev. Sci. Instrum.* **2013**, *84*, 086106 DOI: 10.1063/1.4818977.
(38) Barker, J. R.; Ortiz, N. F.; Preses, J. M.; Lohr, L. L.; Maranzana, A.; Stimac, P. J.; Nguyen, T. L.; Kumar, T. J. D. *MultiWell Program Suite*, version 2014.1b; University of Michigan: Ann Arbor, MI, U.S., 2014; http://aoss-research.engin.umich.edu/multiwell.
(39) Barker, J. R. Multiple-Well, Multiple-Path Unimolecular Reaction Systems. I. MultiWell Computer Program Suite. *Int. J. Chem. Kinet.* **2001**, *33*, 232−245, DOI: 10.1002/kin.1017.
(40) Barker, J. R. Energy Transfer in Master Equation Simulations: A New Approach. *Int. J. Chem. Kinet.* **2009**, *41*, 748−763, DOI: 10.1002/kin.20447.

DOI: 10.1021/acs.jpclett.5b01109
J. Phys. Chem. Lett. 2015, 6, 2708−2713

(41) Basire, M.; Parneix, P.; Calvo, F. Quantum Anharmonic Densities of States Using the Wang-Landau Method. *J. Chem. Phys.* **2008**, *129*, 081101 DOI: 10.1063/1.2965905.
(42) Wang, F.; Landau, D. P. Efficient, Multiple-Range Random Walk Algorithm to Calculate the Density of States. *Phys. Rev. Lett.* **2001**, *86*, 2050 DOI: 10.1103/PhysRevLett.86.2050.
(43) Nguyen, T. L.; Barker, J. R. Sums and Densities of Fully Coupled Anharmonic Vibrational States: A Comparison of Three Practical Methods. *J. Phys. Chem. A* **2010**, *114*, 3718−3730, DOI: 10.1021/jp100132s.
(44) Nguyen, T. L.; Stanton, J. F.; Barker, J. R. A Practical Implementation of Semi-Classical Transition State Theory for Polyatomics. *Chem. Phys. Lett.* **2010**, *499*, 9−15, DOI: 10.1016/j.cplett.2010.09.015.
(45) Pople, J. A.; Head-Gordon, M.; Raghavachari, K. Quadratic Configuration Interaction. A General Technique for Determining Electron Correlation Energies. *J. Chem. Phys.* **1987**, *87*, 5968 DOI: 10.1063/1.453520.
(46) Dunning, T. H.; Hay, P. J. *Modern Theoretical Chemistry*; Springer: Plenum, NY, 1977.
(47) Becke, A. D. Density-Functional Thermochemistry. III. The Role of Exact Exchange. *J. Chem. Phys.* **1993**, *98*, 5648 DOI: 10.1063/1.464913.
(48) Lee, C.; Yang, W.; Parr, R. G. Development of the Colle-Salvetti Correlation-Energy Formula Into a Functional of the Electron Density. *Phys. Rev. B* **1988**, *37*, 785 DOI: 10.1103/PhysRevB.37.785.
(49) Krishnan, R.; Binkley, J. S.; Seeger, R.; Pople, J. A. Self-Consistent Molecular Orbital Methods. XX. A Basis Set for Correlated Wave Functions. *J. Chem. Phys.* **1980**, *72*, 650 DOI: 10.1063/1.438955.
(50) Clark, T.; Chandrasekhar, J.; Spitznagel, G. W.; Schleyer, P. V. R. Efficient Diffuse Function-Augmented Basis Sets for Anion Calculations. III. The 3-21+G Basis Set for First-R3ow Elements, Li−F. *J. Comput. Chem.* **1983**, *4*, 294 DOI: 10.1002/jcc.540040303/pdf.
(51) Frisch, M. J.; Pople, J. A.; Binkley, J. S. Self-Consistent Molecular Orbital Methods 25. Supplementary Functions for Gaussian Basis Sets. *J. Chem. Phys.* **1984**, *80*, 3265 DOI: 10.1063/1.447079.
(52) Frisch, M. J.; Trucks, G. W.; Schlegel, H. B.; et al. *Gaussian 09*, revision A.02, Gaussian, Inc.: Wallingford, CT, 2009.
(53) Werner, H.-J.; Knowles, P. J.; Knizia, G.; et al. *MOLPRO*, version 2010.1, a package of ab initio programs; see http://www.molpro.net.
(54) Ryzhkov, A. B.; Ariya, P. A. A Theoretical Study of the Reactions of Carbonyl Oxide with Water in Atmosphere: The Role of Water Dimer. *Chem. Phys. Lett.* **2003**, *367*, 423 DOI: 10.1016/S0009-2614(02)01685-8.
(55) Ryzhkov, A. B.; Ariya, P. A. The Importance of Water Clusters $(H_2O)_n$ (n = 2, ..., 4) in the Reaction of Criegee Intermediate with Water in the Atmosphere. *Chem. Phys. Lett.* **2006**, *419*, 479 DOI: 10.1016/j.cplett.2005.12.016.

Downloaded by ACADEMIA SINICA on September 3, 2015 | http://pubs.acs.org
Publication Date (Web): June 26, 2015 | doi: 10.1021/acs.jpclett.5b01109

DOI: 10.1021/acs.jpclett.5b01109
J. Phys. Chem. Lett. 2015, 6, 2708−2713